PAPERS

Coherent Control of Chirality in Ensemble of Randomly Oriented Molecules Using a Sequence of Short Laser Pulses[1]

D. V. Zhdanov and V. N. Zadkov

International Laser Center and Faculty of Physics, Moscow State University, Moscow, 119991 Russia

e-mail: zhdanov@phys.msu.ru, zadkov@phys.msu.ru

Abstract—The universal algorithm of choosing the train of short laser pulses, which could selectively excite the specific enantiomers in a racemic mixture of rotationally cold molecules, is proposed. Its application is illustrated on example of laser control of content of different chiral conformations in the mixture of hydrogen peroxide molecules. Methods of detection of racemity breaking in case of dynamical chirality are also discussed.

1. INTRODUCTION

The problem of absolute asymmetric synthesis (AAS) is one of enigmas of the modern molecular science, which still has no general solution despite it is constantly at focus of attention of scientists of different branches of physics, chemistry, biology, and life sciences since 1849 when Louis Pasteur produced a pure sample of levotartaric acid which was the first demonstration of enantiomers of chiral molecule (a pair of isomers which are mirror reflections of each over). The AAS is targeted at formation of an excess of given enantiomer (called sometimes also as "enrichment", "purification" or "distillation") in a racemic (i.e., equally weighted) mixture of enantiomers. The importance of the problem originates from amazing fact of chiral purity of molecules constituting cells of all living beings. Thus, understanding the principles of asymmetric synthesis both casts light on fundamental question of the origin of life and also removes acute shortage of reagents for many practical applications in medicine, chemistry, pharmaceutical and food industries etc. The most vivid examples of a successful solution of the AAS problem are suggested by chemists and are based on a sophisticated choice of chiral catalysts [1]. Although remedying the situation for a few particular cases they however help a little to shine a light on how to solve the problem as a whole.

Therefore, the nowadays hopes are pinned on possible physical ways of realizing the AAS [2]. In particular, recent progress in laser technologies raises an increasing interest to searching the solution among the optical methods, which are incidentally the only physical methods that allow reliable detecting and distinguishing the enantiomers. Nevertheless, among a large number of different theoretical proposals [3, 4] only a few of them have been verified experimentally. Among

them are scenarios of the AAS based on utilization of magneto-chiral effect [5] and electroquadrupole interaction with circularly polarized light [6–9]. Unfortunately, similarly to the case of asymmetric catalysis the necessity in rather specific molecular properties cause these scenarios to have very narrow applicability (in particular, they are deliberately inapplicable to small molecules).

To overcome this shortcoming, it is natural to employ more conventional and widely used mechanisms of laser coherent control of molecular dynamics. That is why many theoreticians look towards elaboration of the AAS driven by pure electrodipole interactions with laser radiation [10–37]. However, none of these scenarios occurs suitable for practical implementation. The most common reasons for that are impracticable assumptions of preliminary molecular orientation (for scenarios developed in [11–27]) or precise spatial localization (for scenarios developed in [31–36] and zero initial temperature of the molecules. Moreover, analysis of the results of the AAS is also a nontrivial problem due to the nonstable (dynamical) character of chirality of almost all sample molecules. In most of the cited above papers the scope of consideration does not go beyond the bounds of particular scheme of excitation, which is often closely locked on a specific target molecule via peculiar limitations on its properties (such as existence of achiral excited electronic states for the scenarios given in [32, 33]).

In our recent paper [38], we made an attempt to systemize and generalize the ideas of laser control of molecular chirality suggested in these works, and derive a number of universal obligatory conditions on the parameters of field-molecule interaction in the AAS scenarios. We also successfully employed these conditions to elaborate a new scheme of the AAS based on the laser-assisted orientation-dependent selection of molecules. In this scheme, we take advan-

---

[1] The article is published in the original.

tages of combined adiabatic and nonadiabatic regimes of interaction with strong multicolor laser pulses. Numerical tests prove that well-known property of stability of adiabatic couplings with respect to variations of the laser pulses parameters allows this scheme to be effective for distillation in a macroscopic part of isotropic gaseous racemate even at room temperature. However, the adiabatic couplings compared to nonadiabatic ones are shown to demand orders of magnitude higher laser intensities and pulse durations [16, 20] and, therefore, in many cases may be unrealizable within sub-breakdown fields strengths or ineffective due to the strong parasitic effects such as photodissociation [26].

In this paper, we will analyze in detail one of the alternative approaches based on a nonadiabatic resonant impact of the sequence of laser pulses of simple form. Various schemes of the AAS of such kind were already elaborated for the case of preliminary oriented molecules [13–26]. However, the case of isotropic racemate is scantily explored, though there exist the particular proposal for the specific case of molecules with achiral excited state [32, 33].

The aim of this work is to generalize the results of the above works and our previous investigations [36, 37] and to elaborate an algorithm of development of the AAS scenarios via action of a train of short laser pulses for the case of randomly oriented molecules bearing on obligatory conditions derived in [38]. Our results also complement the material of [38] with the methodological example of application of these conditions in case of essentially quantum-mechanical character of rapid rotations of small molecules and also with detailed consideration of the case of dynamical chirality. Also the problem of heterogeneous spatial distribution of enantiomeric excess, which is native for all suggested schemes, will be considered in the context of possible ways of detection of induced chiral symmetry breaking. As a computational example of the AAS, the hydrogen peroxide molecule (H_2O_2) will be considered. It is worth to stress, that for many reasons (hardly achievable necessary laser pulses, difficult detection of the signal) this molecule is a poor candidate for the real AAS experiment. But due to its simplicity and availability of detailed data about its structure, this molecule is ideal for both qualitative and quantitative illustrations of the general solution in principle, suggested in this work.

The paper is organized as follows. Section 2 gives a brief insight in theoretical description of molecular chirality and overview of obligatory conditions derived in [38]. Section 3 presents the abstract description of conceptual basics and limitations of proposed general algorithm for construction of the laser-driven AAS scenarios based on illumination of the molecules by trains of short laser pulses. Next two sections illustrate an application of this algorithm on example of hydrogen peroxide molecules. In the auxiliary Section 4, general molecular parameters and peculiarities of

mathematical description of rovibrational dynamics are introduced. In Section 5 the scenario of laser-driven enantiomeric enrichment of racemic H_2O_2 vapor is proposed and analyzed in detail. Possible method of detection of the media symmetry breaking is also discussed. In conclusion, Section 6 summarizes the results of the paper.

2. MATHEMATICAL MODEL OF MOLECULAR CHIRALITY

2.1. Mathematical Background

The mirror mutual correspondence of different enantiomeric forms of a molecule (often called L- and D-forms) means that if we introduce a set of quantum states $|L_k\rangle$ ($k = 1, 2...$), corresponding to L-form of the molecule, then one can simply obtain the corresponding set for the D-form applying spatial inversion operator $\hat{E}^*$:

$$|D_k\rangle = \hat{E}^*|L_k\rangle, \qquad (1)$$

and vise versa. However, it is well-known that the eigen molecular hamiltonian $\hat{H}_0$ (up to negligibly small corrections due to the weak interactions) is invariant with respect to $\hat{E}^*$:

$$\hat{E}^{*^{-1}}\hat{H}_0\hat{E}^* = \hat{H}_0. \qquad (2)$$

Comparing Eqs. (1) and (2) one can deduce that $|L_k\rangle$ can be in fact only approximate eigenstates, while the true eigenstates $|\Psi_k\rangle$ have definite parity: $\hat{E}^*|\Psi_k\rangle = |\Psi_k\rangle$, $\hat{E}^*|\Psi_{-k}\rangle = -|\Psi_{-k}\rangle$. Here each pair of indices of opposite sign enumerates so-called chiral doublet states with identical quantum numbers except parity. It is easy to see that the states $|L_k\rangle$ and $|D_k\rangle$, which correspond to Eq. (1), can be expressed as coherent superposition of states of k-th chiral doublet:

$$|L_k\rangle = \frac{1}{\sqrt{2}}(|\Psi_k\rangle + |\Psi_{-k}\rangle),$$

$$|D_k\rangle = \frac{1}{\sqrt{2}}(|\Psi_k\rangle - |\Psi_{-k}\rangle) \quad (k > 0). \qquad (3)$$

Thus, even without any external influence, the L- and D-molecular conformations should self-interconvert at the time $\tau_{tun} = \pi\hbar/|E_{-k} - E_k|$, where E_k and E_{-k} are the energies corresponding to the states $|\Psi_k\rangle$ and $|\Psi_{-k}\rangle$, respectively. Note that time τ_{tun} varies from a few picoseconds up to few millions of years, depending on the parameters of the potential barrier separating localized chiral states in a particular molecule. In the case of small τ_{tun} (compared with typical time scale of an experiment) it is said about *dynamical* molecular chirality, while other limiting case is designated as *stable* chirality.

To quantify the enantiomeric constitution of a molecular mixture we will use the value χ of relative excess of the *L*-forms of molecule over the *D*-forms ($-1 \leq \chi \leq 1$, $\chi = \pm 1$ correspond to the pure *L/D*-enantiomers). This quantity is often called the degree of chirality and corresponds to following quantum operator:

$$\hat{\chi} = \sum_{k=1}^{\infty} |L_k\rangle\langle L_k| - |D_k\rangle\langle D_k| = \sum_{k=-\infty}^{\infty} |\Psi_k\rangle\langle\Psi_{-k}|. \quad (4)$$

2.2. Obligatory Conditions of Symmetry Breaking

In this work, we will focus on enantiomeric enrichment of an initially racemic mixture of chiral molecules (i.e., ways of controllable breaking the equality $\chi = 0$) by couplings of molecular dipole moment **d** with the complex electric field $\mathcal{E}$ produced by a series of laser pulses $\mathcal{E}_j$:

$$\mathcal{E} = \sum_j \mathcal{E}_j = 2\sum_j \varepsilon_j A_j(t)\cos(\omega_j t + \varphi_j), \quad (5)$$

where $A_j(t)$, ω_j, and ε_j are the envelopes, frequencies, and unit vectors along the polarization of the respective pulses. Mathematically, these couplings can be described via semiclassical additive $\hat{H}_I(\mathcal{E}) = -\mathbf{d}\mathcal{E}$ to the eigen Hamiltonian.

In our previous work [38], we develop an universal theoretical background for elaborating the scenarios of such kind, revealing the set of six symmetry-based conditions on the parameters of field-molecule interaction, which are obligatory for selective excitation of different chiral forms of molecule. In the following we will briefly outline these basic results.

First of all, we have shown that the necessary condition of radiational selectivity is the coherent linkage of the states of the chiral doublets (see Fig. 1):

(i) The selective excitation of enantiomers in the isotropic racemic mixture can be achieved only as a result of *N*-photon processes where *N* is an *odd* number that link coherently the rovibronic states $|\Psi_{\alpha_1}\rangle$ and $|\Psi_{\alpha_{N+1} = -\alpha_1}\rangle$ of the chiral doublets by the chain of dipole transitions through the *even* number of intermediate rovibronic states $|\Psi_{\alpha_p}\rangle$ ($p = 2, 3, ..., N$) (see Fig. 1).[2]

The next two conditions refine the above result for the case of chiral molecules, which rotational dynamics is well-described by the model of rigid rotor (i.e., the object with fixed principal momenta of inertia) with principal axes of inertia directed along unit vectors $\hat{\epsilon}_{x'}$, $\hat{\epsilon}_{y'}$, and $\hat{\epsilon}_{z'}$:

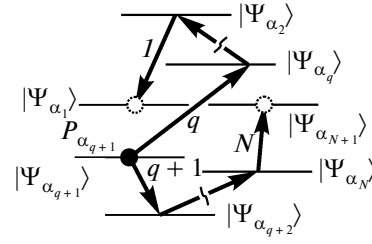[2] The origin of this result is also discussed in [10].

Fig. 1. The laser-induced chain of dipole transitions for the selective excitation of enantiomers.

(ii) Configurational structure of the transition dipole moments of the rovibronic transitions constituting the chain must be noncoplanar.

(iii) Each of the three components $\hat{\epsilon}_{x'}\hat{d}_{x'}$, $\hat{\epsilon}_{y'}\hat{d}_{y'}$, and $\hat{\epsilon}_{z'}\hat{d}_{z'}$ of the dipole moment must be responsible for the odd number of transitions in the chain.

The forth condition clarifies the polarization structure of the incident laser field (5):

(iv) Polarization configuration of the incident radiation should be noncoplanar. Specifically, let us assume that $\mathcal{S}'$ is a set of indices of the *K* laser field components with directions $\varepsilon_{j'}$ of the polarization vectors orthogonal to the plane $\mathcal{S}$ and $N_\perp$ is the number of rovibronic transitions in the chain of transitions induced by these *K* components. Then, $N_\perp$ has to be odd if the directions of polarization vectors of remaining components lie in $\mathcal{S}$.

The following condition deals with the case of heavy molecules and transitory resonant laser excitation when one can neglect both quantum features in rotational dynamics and any classical rotational dislocations of molecules during irradiation. For this case it is possible to introduce the following obligatory criterion for the choice of both polarization of the field components and intermediate vibronic levels in the above chain:

(v) Let us define as $\epsilon_{k,l}^l$ and $\epsilon_{k,l}^d$ the directions of the transition dipole moments of vibronic transitions between *k*-th and *l*-th vibronic states in the molecular frame of *L*- and *D*-molecular conformations corresponding to above chain. Denote as $\varepsilon_{j(\alpha_k, \alpha_l)}$ the polarizations of the field components, driving the corresponding transitions. Then, the following inequality is obligatory for the selective excitation of enantiomers

$$\left\langle \prod_{p=1}^{N} \varepsilon_{j(\alpha_p, \alpha_{p+1})}\epsilon_{\alpha_p, \alpha_{p+1}}^l(\vartheta) \right\rangle_\vartheta - \left\langle \prod_{p=1}^{N} \varepsilon_{j(\alpha_p, \alpha_{p+1})}\epsilon_{\alpha_p, \alpha_{p+1}}^d(\vartheta) \right\rangle_\vartheta \neq 0. \quad (6)$$

Here, $\langle...\rangle_{\vartheta}$ denote orientational statistical averaging across all the Euler angles which should be considered as parameters.

The last aspects considered in [38] are the role of phase-matching between the components $\mathscr{E}_j$ and analysis of spatial distribution of induced degree of chirality. It is found that the leading term in the dependence of the degree of chirality χ' of the excited part of the molecules on their spatial location $\mathbf{r}$ has the form:

$$\chi' \propto \mathrm{Re}\left[e^{i\varphi_0} \prod_{p=1}^{N} e^{i\,\mathrm{sgn}(\omega_{\alpha_p, \alpha_{p+1}})\varphi_{j(\alpha_p, \alpha_{p+1})}} \right], \qquad (7)$$

where $\varphi_j = \varphi_j^0 - \mathbf{k}_j \mathbf{r}$, $\omega_{\alpha_p, \alpha_{p+1}} = \dfrac{1}{\hbar}(E_{\alpha_p} - E_{\alpha_{p+1}})$, and φ_0, φ_j^0 are some position-independent quantities (here the case of stable chirality is assumed). Thus, the typical region of space where one can expect selective excitation of a given form of the molecule has dimensions of typical wavelength of the incident radiation. However, from Eq. (7) the following condition of spatially homogeneous excitation of enantiomers of the same configuration in a macroscopic region can be exactly deduced:

(vi) The incident laser field must consist of a set of two or more subsets (u, v, ...) of the components with different frequencies, such as the wavevectors of all the components in the u-subset are collinear to the direction κ_u ($|\kappa_u| = 1$), and $\kappa_u \neq \kappa_w$ ($u \neq w$). Also, for the components of each subset the following phase matching condition must be fulfilled:

$$\sum_{j(\alpha_p, \alpha_{p+1}) \subset \mathbf{u}}^{N} \mathrm{sgn}(\omega_{\alpha_p, \alpha_{p+1}})\omega_{j(\alpha_p, \alpha_{p+1})} = 0. \qquad (8)$$

3. ENERGETICAL SEPARATION OF ENANTIOMERS: THE GENERAL ALGORITHM

Now we are ready to introduce the universal algorithm for constructing scenarios of energetical separation of enantiomers. The concept of the suggested algorithm directly bears on the above conditions and was prompted by Fig. 1. The algorithm is outlined below:

(1) First, one should choose the chain of electrodipole transitions (see Fig. 1) between rovibronic molecular states linking the initially populated sublevels of the chiral doublets (in Fig. 1 these are the sublevels $|\Psi_{\alpha_1}\rangle$ and $|\Psi_{\alpha_{N+1}}\rangle$) so that conditions (i)–(iii) are satisfied.

(2) Next, the transitions of the chain are enumerated in series according to arbitrary chosen traversal direction as shown in Fig. 1.

(3) Then, laser action should be assumed as a train of nonoverlapping pulses, where each pulse is responsible for the corresponding transition in the chain. The order of pulses should satisfy to enumeration of transitions. For the case shown in Fig. 1 the pulse $\mathscr{E}_{j(\alpha_1, \alpha_2)}$ should come first, the pulse $\mathscr{E}_{j(\alpha_2, \alpha_3)}$ should be the next one etc., so that the pulse $\mathscr{E}_{j(\alpha_N, \alpha_{N+1})}$ will be the final pulse in the sequence.

(4) Thereafter, one should define the polarization of each pulse guiding by conditions (iv).

(5) By perforce of special spatial distribution (homogeneous one inclusive!) of induced degree of chirality one further has to perform the choice of directions of propagation of the pulses guiding by Eq. (7) or condition (vi).

(6) Finally, the amplitudes and durations of the pulses ought to be assigned to tune the areas $S_{j(\alpha_m, \alpha_n)} = \dfrac{2}{\hbar}\varepsilon_{j(\alpha_m, \alpha_n)}\mathbf{d}_{\alpha_m, \alpha_n}\int A_{j(\alpha_m, \alpha_n)}(t)dt$ of the first and last pulses to be equal to $\pi/2$, and the areas of the rest of the pulses to be equal to π.

Let us clarify the functional concept of the resulting control scheme. For clarity and simplicity of further considerations only sublevel $|\Psi_{\alpha_1}\rangle$ in Fig. 1 will be assumed to be initially populated. As result of action of the first pulse, half of the population of the racemic state $|\Psi_{\alpha_1}\rangle$ is transferred into the state $|\Psi_{\alpha_2}\rangle$ resulting in coherent superposition of the form $\dfrac{1}{\sqrt{2}}(|\Psi_{\alpha_1}\rangle + e^{i\varphi^*(t)}|\Psi_{\alpha_2}\rangle)$ ($\varphi^*(t)$ is a time-varying phase). The latter laser π-pulses will transport coherently the molecules excited by the first pulse further along the chain of transitions so that the resulting state of the molecules just before the last pulse will be $\dfrac{1}{\sqrt{2}}(|\Psi_{\alpha_1}\rangle + e^{i\varphi^{**}(t)}|\Psi_{\alpha_N}\rangle)$ ($\varphi^{**}(t)$ is also a time-varying phase). The application of the final $\pi/2$-pulse will raise simultaneously the transitions $|\Psi_{\alpha_1}\rangle \longrightarrow |\Psi_{-\alpha_N}\rangle$ and $|\Psi_{\alpha_N}\rangle \longrightarrow |\Psi_{-\alpha_1}\rangle$. Taking into account the infinitesimality of the matrix elements $\langle L_{\alpha_m}|\hat{\mathbf{d}}|D_{\alpha_n}\rangle$ (the latter is simply the existence condition for the localized chiral conformations) and symmetry properties of the states $|\Psi_{\alpha_m}\rangle$ one can easily prove the approximate equality of the dipole momenta of both these transitions and absence of the essential differences in the transition frequencies. Thus, the effect of the last pulse is twofold: first, half of the population of the state $|\Psi_{\alpha_N}\rangle$ (i.e., a quarter of the total number of the molecules) will be transferred into the state $|\Psi_{-\alpha_1}\rangle$, and, second,
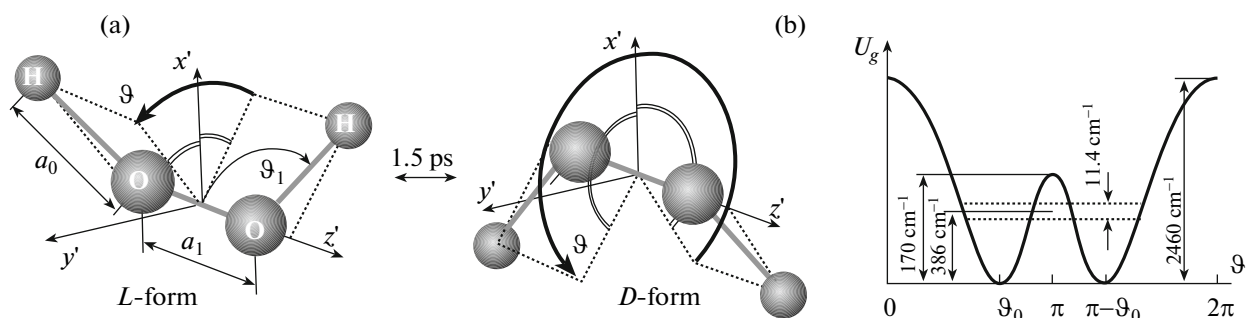
Fig. 2. (a) Geometry of the enantiomers of hydrogen peroxide molecule and molecule-fixed coordinate frame $\{x', y', z'\}$ (axis $\mathbf{x'}$ is parallel to the bisector of dihedral angle $\widehat{HOOH}$). The ground vibronic state parameters are as follows: $\vartheta = 115.16°$ and $244.84°$, $\vartheta_1 = 99°$, $a_1 = 1.451$ Å, $a_0 = 0.962$ Å [41, 42]. (b) Potential energy of the ground state of H_2O_2 as a function of the contorsional coordinate ϑ (see [41]).

half of the molecules in the state $|\Psi_{\alpha_1}\rangle$ (also, a quarter of their total number) will be transferred into the state $|\Psi_{-\alpha_N}\rangle$. Thus, the molecules in α_1th and α_Nth vibronic levels come to be in superposition states $\frac{1}{\sqrt{2}}(|\Psi_{\alpha_1}\rangle \pm |\Psi_{-\alpha_1}\rangle) \equiv \mathrm{sgn}(\alpha_1)|L(D)_{|\alpha_1|}\rangle$ and $\frac{1}{\sqrt{2}}(|\Psi_{\alpha_N}\rangle \mp |\Psi_{-\alpha_N}\rangle) \equiv \mathrm{sgn}(\alpha_N)|D(L)_{|\alpha_N|}\rangle$ (the choice of sign is tuned by the phase matching between the laser pulses). Thereby, the partial racemity of the molecular state in each of these levels becomes broken, i.e., energetical separation of the enantiomers is achieved.[3]

It is important to note two native peculiarities of the proposed scheme, which are the direct consequences of a strict linkage of the chain of transitions, both to preselected rovibronic state and to the appointed intermediate states of a definite symmetry. If the initial state is an incoherent superposition of a large number of different states $|\Psi_{\alpha_m}\rangle$ the laser can excite a wide majority of different chains of transitions satisfying the conditions of energetical separation but with the opposite contributions to the partial degrees of chirality of each vibronic level. Therefore, first, the proposed method is expected to be effective only at the low enough temperatures compared with characteristic values of the molecular rotational constants. Second, the necessity of excitation of the transitions between strongly defined rovibronic states excludes

the possibility of nonresonant excitation of the transitions and also limits the maximum frequency detunings, peak amplitudes, and minimum durations of each pulse in the sequence.

Now let us make the dipper insight into suggested method, familiarizing with it on example of the AAS for hydrogen peroxide molecules.

4. HYDROGEN PEROXIDE—THE SIMPLEST CHIRAL MOLECULE

The hydrogen peroxide molecule (H_2O_2) is a convenient model object for our studies due to its simplicity and availability of both, reach data on its molecular structure [41, 42] and previous investigations of the laser-driven chiral dynamics [36, 37, 43, 44].

Geometry of the enantiomers of H_2O_2 in its ground vibronic state v_0 is shown in Fig. 2a. Like most simplest chiral molecules, these configurations are not stable because of large energetic splitting in the chiral doublets $h\delta_{\mathrm{tun}}^{v_0} \simeq 11.4$ cm^{-1} [41]. Thus, the L- and D-forms mutually interconvert during $\tau_{\mathrm{tun}}^{v_0} \simeq 1.5$ ps.

The substantial feature of the H_2O_2 molecule is existence of a single dominant transformation channel between the chiral isomers of the molecule: the conformations are changed as a result of enlarging the dihedral angle $\widehat{HOOH}$ from $115.16°$ to $244.84°$ without essential alteration of other valent angles and bond lengths (Fig. 2a). The latter gives a possibility to describe the molecular chirality using one-dimensional Hund model [45]. Recall that this model assumes the potential energy surface to have two symmetrically spaced minima along some contorsional coordinate. The wavepackets localized in each of these wells correspond to the distinct chiral conformations whereas the properties of the potential barrier between the wells define the self-interconversion time.

---

[3] Note that the laser impact will lead to the same result also in the case of initial state being the arbitrary noncoherent superposition of the states $|\Psi_{\alpha_1}\rangle$ and $|\Psi_{\alpha_{-1}}\rangle$. In the latter case, the parallel excitation of one more chain of transitions will occur. This chain starts from the state $|\Psi_{\alpha_{-1}}\rangle$ and consists of all the levels $|\Psi_{\alpha_k}\rangle$ with indices k coinciding with the level indices of the considered above chain taken with reversed signs.

Table 1. The lowest vibrational-contorsional levels of the ground electronic state of H_2O_2 molecule [42]

Mode index	Mode description	Energy of the lowest symmetric contorsional state $\lvert...^{(s)}\rangle$ (cm^{-1})	Energy of the lowest antisymmetric contorsional state $\lvert...^{(a)}\rangle$ (cm^{-1})
ν_0	Ground vibrational state	0	11.4
ν_1	Symmetric valent vibrations of hydrogen atoms	3609.8	3618.0
ν_2	Symmetric torsion vibrations (changing the angles $\angle OOH$)	1395.9	1398.3
ν_5	Antisymmetric valent vibrations of hydrogen atoms	3610.7	3618.8

Such a contorsional coordinate in the case of hydrogen peroxide is designated as $\vartheta = \widehat{HOOH}$, and the corresponding two-well potential is sketched in Fig. 2b. From Fig. 2b it is evident that the molecular eigenstates can be splitted into pairs of closely spaced levels $\lvert\nu^{(s)}\rangle$ and $\lvert\nu^{(a)}\rangle$ (here index ν indicates other quantum numbers describing vibronic state), which are symmetric and antisymmetric on ϑ, correspondingly. Thereby, the quasistable chiral states localizing in "left" and "right" wells are described by the following superpositions:

$$\lvert\nu^{(l)}\rangle = \frac{1}{\sqrt{2}}(\lvert\nu^{(s)}\rangle + \lvert\nu^{(a)}\rangle),$$
$$\lvert\nu^{(d)}\rangle = \frac{1}{\sqrt{2}}(\lvert\nu^{(s)}\rangle - \lvert\nu^{(a)}\rangle). \qquad (9)$$

Despite close connection between Eqs. (3) and (9) it must be emphasized that the vibronic states $\lvert\nu^{(s)}\rangle$ and $\lvert\nu^{(a)}\rangle$ should not be confused with *rovibronic* states $\lvert\Psi_k\rangle$ and $\lvert\Psi_{-k}\rangle$. In particular, contrary to the latter ones, the states $\lvert\nu^{(s)}\rangle$ and $\lvert\nu^{(a)}\rangle$ have not definite symmetry with respect to the inversion operation $\hat{E}^*$ unless the symmetry of rotational state is exactly specified. Nevertheless, the states $\lvert\nu^{(s)}\rangle$ and $\lvert\nu^{(a)}\rangle$ are sufficiently more useful for description of chiral dynamics, especially in the case of dynamic chirality, because their structure is well-adopted for description of the tunneling effects in

Table 2. Properties of several vibrational dipole transitions for L-enantiomer of H_2O_2 molecule calculated using results of [42]

Vibrational transition	Approximate values ($\pm25\%$) of x'-, y'-, and z'-components of transition dipole momenta [D]
$\lvert\nu_0^{(l)}\rangle \longleftrightarrow \lvert\nu_1^{(l)}\rangle$	{0.51, 0, 0}
$\lvert\nu_0^{(l)}\rangle \longleftrightarrow \lvert\nu_5^{(l)}\rangle$	{0, 0.51, 0.13}
$\lvert\nu_0\rangle^{(l)} \longleftrightarrow \lvert\nu_2^{(l)}\rangle$	{0.14, 0, 0}
$\lvert\nu_1\rangle^{(l)} \longleftrightarrow \lvert\nu_2^{(l)}\rangle$	{0.094, 0, 0}

specific molecules and for splitting of vibrational, rotational, and contorsional variables. That is why we will rest upon these states through the rest of the paper.

We will elaborate the method of coherent control of molecular chirality based on the subsequent excitation of the different lowest vibrational modes of the lowest contorsional doublet and the ground electronic state of H_2O_2 molecule. Brief description of the properties of several lowest vibrational modes and dipole transitions, which will be used in our control scenario, are given in Tables 1 and 2 for reference. In particular, from Table 1 one can see that doublet splittings between the lowest contorsional states and thereby the times of self-interconversion between the chiral conformations are strongly dependent on vibrational state of the molecule.

The important advantage of hydrogen peroxide as a model molecule for theoretical analysis is the feasibility of several substantial simplifications in the rotational dynamics description. First, note that due to the substantive differences in masses of O and H atoms the directions of principal inertia axes are close to directions of the frame axes $\mathbf{x'}$, $\mathbf{y'}$, $\mathbf{z'}$ shown in Fig. 2. Moreover, the corresponding approximate principal momenta of inertia $I_{x'}$, $I_{y'}$, and $I_{z'}$ satisfy relations $I_{x'} \simeq I_{y'} \gg I_{z'}$ and negligibly depend on contorsional and vibrational state. Thus, the rotational dynamics of the molecule, despite its essential nonrigidity, can be rather accurately described within the rigid symmetric top model with $\mathbf{z'}$ taken as its axis (e.g., corresponding errors in the rotational energies for the angular momentum $J \leq 3$ do not exceed 0.1%). We should stress, however, that in this simple approximation we lose the possibility of correct account of selection rules caused by indistinguishability of identical particles (for such an account the choice of axis $\mathbf{x'}$, which is the symmetry axis of the second order, as a quantization axis would be preferable). Thus, the H_2O_2 molecule can be treated as a rigid rotor and thus falls within the scope of the obligatory conditions of Subsection 2.2. The latter proves the feasibility of applying the algorithm proposed in previous section to this molecule.

Keeping in mind that our consideration is aimed only at demonstration the proposed solution in principle, we will make one more severe assumption arising

from large difference (about an order of magnitude) between the characteristic classical frequency of molecular rotation around the $\mathbf{z'}$ axis and analogous frequencies for the two another axes. Note that for the rotational temperature lower than $10-15$ K the typical classical period of rotations around the latter axes does not fall below the few picoseconds. Thus, with the use of the pulse sequences of picosecond duration we can additionally assume the direction of the axis $\mathbf{z'}$ to be rotationally "frozen" during the laser illumination. As a result, we come to our main reduced one-dimensional model of molecular rotations, in which the only dynamical variable is the Euler angle γ describing the rotations around axis $\mathbf{z'}$ (corresponds to the quantum number k of the angular momentum projection on this axis) whereas remaining rotational degrees of freedom (i.e., angles α and β), characterizing the direction of $\mathbf{z'}$, are treated as parameters. Thus, the consideration of laser impact on chaotically oriented molecules in the frame of this model among quantum-mechanical computations includes subsequent statistical averaging over two angular parameters.

Let us turn now to elaboration of scenario of the laser-driven AAS, using the above data and approximations.

5. LASER COHERENT CONTROL OF DYNAMIC CHIRALITY IN H_2O_2 MOLECULES

First of all, let us flesh out our problem settling. Suppose that initially we have a racemic mixture of free noninteracting H_2O_2 molecules at zero rotational temperature. As the initial vibrational-contorsional state we will take the incoherent superposition of equally populated states $|\nu_0^{(s)}\rangle$ and $|\nu_0^{(a)}\rangle$. Our main task will be searching for the laser action, which could raise the excess of predefined enantiomer (at a given time instant) in a specific point of space. It must be emphasized that we will not demand the carrying-out of condition (vi) of achieving the enantiomeric excess of the same enantiomer simultaneously in a macroscopic region of space because such additional complication seems to be inexpedient in the case of molecules possessing the fast oscillating dynamical chirality.

As it happens, the solution of the task can be obtained simply via energetical separation of different enantiomeric forms between two vibrational levels with the distinct doublet splitting δ_{tun} between its chiral sublevels. Consider, for example, the levels ν_0 and ν_2 ($\delta_{\mathrm{tun}}^{\nu_0} = 342$ GHz, $\delta_{\mathrm{tun}}^{\nu_2} = 72$ GHz). Suppose that in a certain point of space at the time instant $t = 0$ the chiral conformations were energetically separated via selective population of vibrational state ν_2 in a number of molecules in D-conformation. Thus, the

partial contributions χ^{ν_0} and χ^{ν_2} of the states ν_0 and ν_2 into the local degree of chirality χ becomes nonzero: $\chi^{\nu_0}(t) = \frac{1}{2}\chi_0\cos(2\pi\delta_{\mathrm{tun}}^{\nu_0}t)$ and $\chi^{\nu_2} = -\frac{1}{2}\chi_0\cos(2\pi\delta_{\mathrm{tun}}^{\nu_2}t)$. The value of χ_0 here is proportional to the number of excited molecules and oscillating terms describing the tunneling between the different enantiomeric forms. Due to the distinct oscillation frequencies, the overall local degree of chirality takes the form:

$$\chi(t) = \chi^{\nu_0}(t) + \chi^{\nu_2}(t)$$
$$= \chi_0\cos(2\pi(\delta_{\mathrm{tun}}^{\nu_0} - \delta_{\mathrm{tun}}^{\nu_2})t/2)\cos(2\pi(\delta_{\mathrm{tun}}^{\nu_0} + \delta_{\mathrm{tun}}^{\nu_2})t/2). \tag{10}$$

Thus, the value of χ is still equal to zero at $t = 0$, but becomes nonzero at the latter time moments varying accordingly with the biharmonic law with the peak amplitude χ_0.

To elaborate the scenario of energetical separation, we used the algorithm from Section 3 and the data listed in Tables 1 and 2 with additional request of the low number of "links" in the chain of transitions and large enough values of all the employed transition dipole momenta. The resulted proposal is shown in Fig. 3. The laser action is composed of three laser pulses $\mathscr{E}_1$, $\mathscr{E}_2$, and $\mathscr{E}_3$ with the different carrier frequencies, propagating along two mutually orthogonal directions κ_1 and κ_2, as shown in Fig. 3b. From Fig. 3c, however, one can see that the corresponding chain of transitions consists of not three but five links because the first pulse $\mathscr{E}_1$ excites the first three transitions simultaneously. Using Fig. 3b one can easily verify the fulfilment of the conditions of oddness of transitions in the chain, noncoplanarity of polarization configuration of the laser field, and condition (iv) for each of the planes xz, yz, and xy chosen as plane $\mathscr{S}$.

The configuration of the matrix elements of the dipole momenta for employed rovibrational transitions is shown in Fig. 3a. After the first look on the figure, a thorough reader could wonder whether the shown configuration really satisfies the noncoplanarity condition (ii). Indeed, the directions of the dipole momenta of all the vibrational transitions belong to the same plane defined by vectors $\mathbf{x'}$ and $\mathbf{d}_{\nu_0, \nu_5}$. Thus, be molecules "glued" and immobilized, the proposed scheme would be unable to work due to evident violation of the condition (v). However, in the previous section, we have seen that at the laser interaction durations of the picosecond time scale one have to take into account at least the fast rotations of molecules around the axis $\mathbf{z'}$. It is now evident that we are beyond the scope of applicability of the "frozen" approximation and condition (v) and obliged to perform exact consideration of transitions between the distinct rotational-vibrational sublevels. Note that condition (ii)
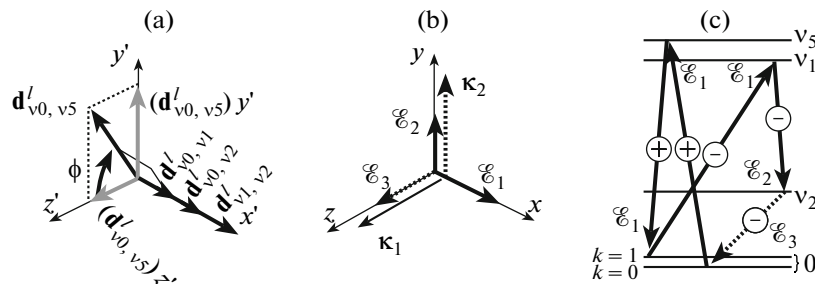
Fig. 3. The laser control scenario of the AAS for randomly oriented hydrogen peroxide molecules. (a) Configuration of the employed transition dipole momenta (see also Tables 1 and 2). (b) Polarizations and directions of propagation (κ_1 and κ_2) of the laser pulses. The constituents $\mathcal{E}_1$ and $\mathcal{E}_2$ of the first pulse are shown by solid arrows, while the single component $\mathcal{E}_3$ of the second pulse along with its direction of propagation are shown by dashed arrows. (c) The laser-driven chain of transitions. Signs "−" and "+" indicate whether or not particular transition results in change of the state symmetry with respect to the contorsional coordinate.

was derived exactly for such detailed level of consideration. It can be shown that the dipole momenta of rovibrational transitions in the case of rigid-rotor-like molecules are always collinear to its principal axes of inertia [38]. Thus, even in a reduced one-dimensional model of rotations the z'- and y'-projections of the dipole moment of vibrational transition $\nu_0 \longleftrightarrow \nu_5$ (shown in Fig. 3b by grey arrows) produce the distinct "links" for the chain of transitions: in the first case there is no changes of the quantum number k occur whereas $\Delta k = \pm 1$ in the second one. Suppose that the first two links in the chain shown in Fig. 3c are excited by different projections of $\mathbf{d}_{\nu_0, \nu_5}$. Then the effect of the corresponding two-photon transition is that despite the molecules return back into its initial vibrational state, it still appear in the new rotational state with $|k| = 1$. Using Fig. 3a one can easily prove now that such transition chain satisfy both conditions (ii) and (iii). Thus, we are assured that proposed scenario satisfy all the necessary conditions of energetical separation.
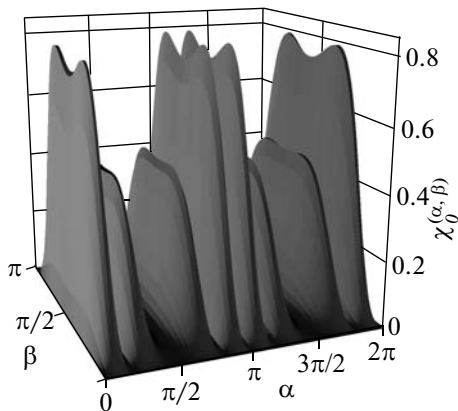

Fig. 4. Dependence of the local amplitude $\chi_0^{(\alpha, \beta)}$ photoinduced chirality on the Euler angles α and β for the optimal parameters of the laser impact (see the text).

To quantify the efficacy of the proposed scenario let us estimate the achievable amplitude χ_0 of local photoinduced oscillations of the degree of chirality [Eq. (10)]. To do this, we will first calculate in frame of one-dimensional model of rotations the peak degrees of chirality $\chi_0^{(\alpha, \beta)}$ produced by the laser pulses in each local subensemble of molecules having the same orientation of axis $\mathbf{z}'(\alpha, \beta)$ and then will perform the averaging over such subensembles: $\chi_0 = \langle \chi_0^{(\alpha, \beta)} \rangle_{\alpha, \beta}$.

It is turned out that it is possible to derive an analytical expression for $\chi_0^{(\alpha, \beta)}$ under several extra assumptions:

• suppose that laser pulses do not overlap;

• relaxation and intermode interaction can be neglected;

• equilibrium values of contorsional coordinate for all the employed states $|\nu_m^l\rangle$ and $|\nu_m^d\rangle$ are roughly estimated as $\vartheta = 90°$ and $270°$, correspondingly;

• laser pulses frequencies are resonant to the corresponding transitions shown in Fig. 3c;

• calculations can be done within the bounds of rotation wave approximation;

• all the nonresonant transitions can be neglected.

In frame of the last assumption we account for only the dipole transitions detuned less than 30 cm^{-1} from the resonance (neglecting the corresponding detunings itself). Practically, it means that the levels with $k < 2$ only are to be included in calculations. This assumption is rather correct unless the laser pulses durations are below the picosecond scale.

Simple but cumbersome computation shows that within above assumptions the value of $\chi_0^{(\alpha, \beta)}$ does not explicitly depend on the envelope shapes and durations of the pulses (see Eq. (5)), but can be expressed in terms of their integral characteristics $s_j = \int A_j dt$ ($j = 1, 2, 3$):

$$\chi_0^{(\alpha,\beta)} = 2\mathfrak{d}_{0,1}^{(1,x')}\mathfrak{d}_{0,5}^{(1,y')}\mathfrak{d}_{0,5}^{(1,z')}$$

$$\times\left[\sin\frac{s_1\sqrt{\mathfrak{D}_2-\mathfrak{D}_1}}{\sqrt{2}}\sqrt{\mathfrak{D}_1+\mathfrak{D}_2}\left(\mathfrak{D}_1-\frac{1}{2}(\mathfrak{d}_{0,1}^{(1,x')})^2\right)\right.$$

$$\left.+\sin\frac{s_1\sqrt{\mathfrak{D}_1+\mathfrak{D}_2}}{\sqrt{2}}\sqrt{\mathfrak{D}_2-\mathfrak{D}_1}\left(\frac{1}{2}(\mathfrak{d}_{0,1}^{(1,x')})^2+\mathfrak{D}_1\right)\right]$$

$$\times[\sqrt{2}\mathfrak{D}_1^2\sqrt{\mathfrak{D}_2^2-\mathfrak{D}_1^2}]^{-1} \quad (11)$$

$$\times\sin\left(\frac{1}{\sqrt{2}}s_2\mathfrak{d}_{1,2}^{(2,x')}\right)\sin(\sqrt{2}s_3\mathfrak{d}_{0,2}^{(1,x')})$$

$$\times\left(\cos\frac{s_1\sqrt{\mathfrak{D}_2-\mathfrak{D}_1}}{\sqrt{2}}-\cos\frac{s_1\sqrt{\mathfrak{D}_1+\mathfrak{D}_2}}{\sqrt{2}}\right)$$

$$\times\sin(\varphi_1-\varphi_2-\varphi_3).$$

In this expression we used decomposition of the dipole moment operator introduced while formulating the condition (iii), and also the following notations:

$$\mathfrak{d}_{m,n}^{(j,\xi)} = \frac{1}{\hbar}(\boldsymbol{\varepsilon}_j\boldsymbol{\epsilon}_\xi)\langle\nu_m^{(l)}|\hat{d}_\xi|\nu_n^{(l)}\rangle,$$

$$\mathfrak{D}_1(\alpha,\beta) = \sqrt{\frac{1}{4}(\mathfrak{d}_{0,1}^{(1,x')})^4+8(\mathfrak{d}_{0,5}^{(1,y')})^2(\mathfrak{d}_{0,5}^{(1,z')})^2},$$

$$\mathfrak{D}_2(\alpha,\beta) = \frac{1}{2}(\mathfrak{d}_{0,1}^{(1,x')})^2+(\mathfrak{d}_{0,5}^{(1,y')})^2+2(\mathfrak{d}_{0,5}^{(1,z')})^2.$$

The results of numerical averaging of the $\chi_0^{(\alpha,\beta)}$ over all possible directions of molecular axis $\mathbf{z}'$ for different values of s_1, s_2, and s_3 confirm that locally averaged amplitude χ_0 is, in general, also nonzero. Its peak value $\langle\chi_0\rangle \sim 0.23$ corresponds to the following parameters: $s_1 = 6\times10^{-4}$ V s/m, $s_2 = 1.4\times10^{-2}$ V s/m, $s_3 = 4.5\times10^{-4}$ V s/m, $\varphi_1-\varphi_2-\varphi_3 = \pi/2$.

It is interesting to take a look at the corresponding dependence $\chi_0^{(\alpha,\beta)}$ shown in Fig. 4. One can see that the orientation of the axis $\mathbf{z}'$ affects only the amplitude of $\chi_0^{(\alpha,\beta)}$, not its sign. Thus, the asymmetric synthesis proceeds with essentially different efficacy, but in the same direction independently of orientation of the molecules. Note also that several particular orientations of molecular axis $\mathbf{z}'$ correspond to very large amplitudes of $\chi_0^{(\alpha,\beta)}$ up to 0.8. Thus, the efficacy of the proposed scenario of AAS in partially oriented molecules is comparable with the efficacy of the previously suggested scenarios of AAS specifically designed for the entirely preoriented molecules [11−24].

The simple and visual dynamical model described above is however rather questionable due to the large number of arguable suppositions. So, to verify the reli-

ability of the results we complement the above calculations with ones made in fully numerical manner using more accurate totally quantum-mechanical three-dimensional description of rotations in the frame of a symmetric top model with both extended calculation basis (all the levels with $J < 4$ were included) and explicit account of all detunings from resonance. Note that such an account of detunings raises the dependence of results of laser impact on shape and duration of the laser pulses and requires to be attended by their exact specification. For our calculations we choose the simplest model of rectangular nonoverlapping pulses coursed each other with zero time delays.

Results of our calculations confirm that our previous simple model allows rather satisfactory estimates of optimal parameters s_j which however are somewhat understated (by a factor of 1.35 for s_1 and 1.25 for s_2) over predictions given by more precise calculations. As expected, the optimal pulse durations τ_j are found to be in the picosecond range: $\tau_1 = 1.2$ ps, $\tau_2 = 1.65$ ps, $\tau_3 = 1$ ps (corresponding pulse intensities are 8.7×10^{10}, 1.5×10^{13}, and 1.9×10^{10} W/cm^2, respectively). At the same time, the simple model substantially overestimates the extremal value of χ_0 (0.23 instead of 0.12). Nevertheless, one can conclude that the mutual agreement between the results of two calculations is quite satisfactory.

Let us conclude the discussion with several remarks on possible ways of experimental revealing of the effect of the AAS in the case of dynamical chirality. The simplest method is possibly the detection of constituents of nonlinear response of molecular ensemble to laser impact caused by chiral symmetry breaking.

The idea of the method is the following. Recall that our controlling laser field consists of two groups of pulses propagating in the mutually orthogonal directions $\boldsymbol{\kappa}_1$ and $\boldsymbol{\kappa}_2$, as shown in Fig. 3b. Now let us consider the macroscopic molecular ensemble localized in the finite volume. It is evident that the time delay Δt between arrival of pulses from distinct groups (specifically, between the pulses $\mathcal{E}_2$ and $\mathcal{E}_3$) has to be different for the molecules located in different parts of the volume. This, certainly, raises the spatial dependence of the results on laser impact. For example, the dependence of partial chirality χ^{ν_0} of molecules in the ground vibrational state ν_0 (the expression for χ^{ν_2} is identical) on spatial point $\mathbf{r}$ of their localization in the frame of assumptions of the simple model reads as

$$\chi^{\nu_0}(\mathbf{r},t) = \chi_0^{\nu_0}\cos[2\pi\delta_{\mathrm{tun}}^{\nu_0}t-(\mathbf{k}_1-\mathbf{k}_2-\mathbf{k}_3)\mathbf{r}+\phi]. \quad (12)$$

Here, $\mathbf{k}_j$ is the wavevector of j-th pulse and ϕ is a phase shift, which within the constraints of a simple model is independent on $\mathbf{r}$ and t. Note that described above more precise calculations revealed the slight (as compared to $(\mathbf{k}_1-\mathbf{k}_2-\mathbf{k}_3)\mathbf{r}$ term) dependance of ϕ and,
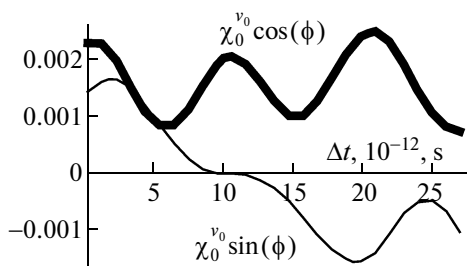
Fig. 5. The dependence of amplitude and phase of the laser-induced oscillations of the averaged local degree of chirality on time delay Δt between the pulses $\mathscr{E}_2$ and $\mathscr{E}_3$ (this estimate was made for the initial temperature $T = 300$).

thus, $\chi_0^{v_0}$ on Δt (see Fig. 5). Figure 5 shows that assumption of the constant ϕ is satisfactory fulfilled for the delays Δt up to 30 ps, i.e., in space areas with characteristic dimensions less than ~1 cm.

It follows from Eq. (12) that the spatial distribution of local degree of chirality at any time instant has the configuration of running spatial grid. Let us show that this grid-like laser-induced chiral asymmetry can be revealed via the effects accompanying the propagation of the tail of the last laser pulse $\mathscr{E}_3$ through the mixture of enantiomers which certainly are already energetically separated to that moment. It can be shown that such an interaction affects the component Q_{yz} of the molecular quadrupole moment Q which begins to oscillate according to following law:

$$Q_{yz} \propto \cos(\omega_3 t - \mathbf{k}_3 \mathbf{r} + \varphi_3)$$
$$\times \cos(2\pi \delta_{tun}^{v_0} t - (\mathbf{k}_1 - \mathbf{k}_2 - \mathbf{k}_3)\mathbf{r} + \phi) \quad (13)$$
$$= \cos((\omega_3 + 2\pi \delta_{tun}^{v_0})t - (\mathbf{k}_1 - \mathbf{k}_2)\mathbf{r} + (\phi + \varphi_3)) + \dots.$$

In view of the fact that $|\mathbf{k}_1 - \mathbf{k}_2| \simeq |\mathbf{k}_3|$, it is easy to see from (13) that oscillations of Q_{xy} up to small detuning $2\pi \delta_{tun}^{v_0}$ [4] are spatially phase-matched to amplify the signal response wave with the frequency $\omega_{signal} = \omega_3 + 2\pi \tilde{\nu}_{v_0}$ polarized parallel to the axis **y** and running along the axis **z**. Origination of this signal wave can be treated as indication of the racemity breaking. Phenomenologically, the appearance of the signal wave can be interpreted as a result of media symmetry breaking with respect to the inversion operation $\hat{E}^*$. First, the signal wave can be treated as a result of emerging the even-order susceptibilities, which lead to generation of the wave with the difference frequency

$\sim(\omega_1 - \omega_2) = \omega_3$ of the pulses $\mathscr{E}_1$ and $\mathscr{E}_2$. Another explanation of the signal wave is that it is a result of scattering of the last pulse $\mathscr{E}_3$ by running a grid of the spatial molecular chirality distribution. This latter explanation seems to be physically more adequate.

Unfortunately, application of the described scheme to the case of hydrogen peroxide molecules seems to be extremely difficult. One of the reasons is mentioned in the final part of Section 3 and raised by strong decrease of effectiveness of the proposed scenario at nonzero initial temperature of molecules. In particular, our estimates show that the amplitude of the local degree of chirality induced in the sample at room temperature is expected to be less than 10^{-3}. On the other hand, preliminary deep cooling of the molecules, e.g., in a supersonic jet, could drastically affect the number of exposed molecules. In any case, the peak intensity of the response signal will be by many orders of magnitude lower than the intensity of the incident laser field. For example, let us consider the case of H_2O_2 molecules at normal conditions. From Fig. 5 one can see that the spatial dependence (5) of partial chirality distribution holds on only in the volume with the dimensions about 1 cm. However, our estimates show that even illumination of this maximal volume cannot result in the peak intensity of the response signal exceeding 10^{-8} W/cm^2.

Another problem arises from strong sensitivity of the results of the laser impact on the laser pulses parameters. For instance, 20% variation of the intensity of the first pulse $\mathscr{E}_1$ leads both to half as much decrease of amplitude χ_0 and to shift by π of the phase of oscillations of the degree of chirality. Thus, the effective generation of the response signal is possible only if the given-field approximation is valid for incident laser field and also if the cross-section intensity distribution of the pulses on the scales of the reaction volume can be neglected.

Finally, it is necessary to stress that during the above consideration we neglected the effects of tunnel ionization, which can be unwarrantable for the obtained optimal intensities and durations of the laser pulses.

6. CONCLUSIONS

In conclusion, we proposed universal algorithm for construction of the schemes of selective laser excitation of given enantiomers for arbitrary randomly oriented chiral molecules which was further successfully applied to the problem of absolute asymmetric synthesis on example of rotationally cold hydrogen peroxide molecules. Specifically, we considered the method of producing the local enantiomeric excess in a racemic mixture of dynamically chiral molecules via energetical separation of enantiomers. We showed that the sequence of three strong (with peak intensities of about $\sim 10^{10} - 10^{13}$ W/cm^2) ps laser pulses with frequencies in the mid-IR range can stimulate the oscillations

---

[4] This detuning can be compensated via the slight declination (on the order of 0.05 rad) between directions of propagation of the pulses $\mathscr{E}_1$ and $\mathscr{E}_2$ or by replacing the pulse $\mathscr{E}_1$ with the pair of pulses of the same frequency with slightly distinct wavevectors directions.

of the degree of chirality with an amplitude of up to 0.12. These results, thus, confirm usefulness and effectiveness of the proposed algorithm as the base for developing the control schemes. Also, we proposed a method for detection of produced nonuniform distribution of chiral content based on the registration of nonlinear response of the media.

Analysis of the hydrogen peroxide molecule case shows that the correct description of the laser-driven chiral dynamics needs an explicit quantum-mechanical consideration of almost all vibrations as well as the molecular rotations because the degrees of freedom of both types hold important information about symmetry properties of interaction. Nevertheless, we found that all the key features of the laser-driven dynamics can be satisfactory reproduced within a simple semi-classical model of rotations. Moreover, in the frame of this model we have been able to rather accurately determine the optimal properties of the laser impact, although obtained twice overestimated values for the peak local degree of chirality compared to the direct quantum-mechanical computations using symmetric top approximation. We also revealed that our scenario allows achieving very high enantiomeric excess $\chi \gtrsim 0.8$ in the case of partly oriented molecules (with only one fixed axis).

At the same time, it is necessary to stress the weaknesses of the proposed scenario. First, the specific scenario for hydrogen peroxide molecules employs the laser pulses with both experimentally hardly achievable frequencies and also extremely high amplitudes, which can raise strong parasitic tunnel ionization. However, these shortcomings are not of fundamental nature and could be eliminated by replacing the rovibrational transitions with rovibronic ones. Unfortunately, there exist a more principal weaknesses, which is native for all the schemes of considered type. Namely, the result is qualitatively changed by rather slight (about $10-20\%$) variations of amplitudes of constituents of the laser impact and effectiveness of the method drastically breaks up at nonzero initial temperatures of molecules. These weaknesses turn the registration of the effect of asymmetric synthesis in H_2O_2 vapor to a very challenging task due to the weakness of the response signal (below 10^{-8} W/cm^2 at normal temperature and pressure of the sample).

ACKNOWLEDGMENTS

REFERENCES

1. Nobel Prize in Chemistry for 2001 was awarded for the development of catalytic asymmetric synthesis, with one half jointly to William S. Knowles and Ryoji Noyori "for their work on chirally catalysed hydrogenation reactions" and the other half to K. Barry Sharpless "for his work on chirally catalysed oxidation reactions."

2. P. Compain, V. Desvergnes, C. Ollivier, et al., New J. Chem. **30**, 823 (2006).

3. L. D. Barron, Chem. Soc. Rev. **15**, 189 (1986).

4. M. Avalos, R. Babiano, P. Cintas, et al., Chem. Rev. **98**, 2392 (1998).

5. G. L. J. A. Rikken and E. Raupach, Nature **405**, 932 (2000).

6. N. P. M. Huck, W. F. Jager, B. Lange, et al., Science **273**, 1686 (1996).

7. Y. Shimizu and S. Kawanishi, Chem. Commun. 1333 (1996).

8. Y. Shimizu, J. Chem. Soc., Perkin Trans. **1**, 1275 (1997).

9. H. Nishino, A. Nakamura, and Y. Inoue, J. Chem. Soc., Perkin Trans. **2**, 1693 (2001); A. Nakamura, H. Nishino, and Y. Inoue, J. Chem. Soc., Perkin Trans. **2**, 1701 (2001); H. Nishino, A. Nakamura, H. Shitomi, et al., J. Chem. Soc., Perkin Trans. **2**, 1706 (2001).

10. M. Shapiro and P. Brumer, Rep. Prog. Phys. **66**, 859 (2003).

11. Y. Fujimura, L. Gonzàlez, K. Hoki, et al., Chem. Phys. Lett. **306**, 1 (1999).

12. K. Hoki, Y. Ohtsuki, and Y. Fujimura, J. Chem. Phys. **114**, 1575 (2001).

13. L. Gonzàlez, K. Hoki, D. Kröner, et al., J. Chem. Phys. **113**, 11134 (2000).

14. M. Shapiro, E. Frishman, and P. Brumer, Phys. Rev. Lett. **84**, 1669 (2000).

15. D. Gerbasi, M. Shapiro, and P. Brumer, J. Chem. Phys. **115**, 5349 (2001).

16. L. Gonzàlez, D. Kröner, and I. R. Sola, J. Chem. Phys. **115**, 2519 (2001).

17. A. S. Leal, D. Kröner, and L. Gonzàlez, Eur. Phys. J. D **14**, 185 (2001).

18. K. Hoki, L. Gonzàlez, and Y. Fujimura, J. Chem. Phys. **116**, 2433 (2002).

19. K. Hoki, L. Gonzàlez, and Y. Fujimura, J. Chem. Phys. **116**, 8799 (2002).

20. Y. Ohta, K. Hoki, and Y. Fujimura, J. Chem. Phys. **116**, 7509 (2002).

21. E. Frishman, M. Shapiro, and P. Brumer, J. Phys. B: At. Mol. Opt. Phys. **37**, 2811 (2004).

22. K. Hoki, D. Kröner, and J. Manz, Chem. Phys. **267**, 59 (2001).

23. D. Kröner, M. F. Shibl, and L. Gonzàlez, Chem. Phys. Lett. **372**, 242 (2003).

24. D. Kröner and L. Gonzàlez, Chem. Phys. **298**, 55 (2004).

25. D. Kröner and L. Gonzàlez, Chem. Phys. **5**, 3933 (2003).

26. K. Hoki, L. Gonzàlez, M. F. Shibl, et al., J. Phys. Chem. A **108**, 6455 (2004).

27. L. Gonzàlez, J. Manz, B. Schmidt, and M. F. Shibl, Chem. Phys. **7**, 4096 (2005).

28. P. Brumer, E. Frishman, and M. Shapiro, Phys. Rev. A **65**, 015401 (2001).

29. S. S. Bychkov, B. A. Grishanin, and V. N. Zadkov, JETPH **116**, 31 (2001).

30. S. S. Bychkov, B. A. Grishanin, and V. N. Zadkov, Las. Phys. **11**, 1088 (2001).

31. P. Král and M. Shapiro, Phys. Rev. Let. **87**, 183002 (2001).

32. E. Frishman, M. Shapiro, D. Gerbasi, et al., J. Chem. Phys. **119**, 7238 (2003).

33. D. Gerbasi, M. Shapiro, and P. Brumer, J. Chem. Phys. **124**, 074315 (2006).

34. P. Král, I. Thanopulos, M. Shapiro, et al., Phys. Rev. Lett. **90**, 033001 (2003).

35. I. Thanopulos, P. Král, and M. Shapiro, J. Chem. Phys. **119**, 5105 (2003).

36. Yu. V. Vladimirova, B. A. Grishanin, D. V. Zhdanov, and V. N. Zadkov, Moscow Univ. Phys. Bull., No. 6, 37 (2005).

37. B. A. Grishanin, H. Takahashi, Yu. V. Vladimirova, D. V. Zhdanov, and V. N. Zadkov, Las. Phys. **15**, 1247 (2005).

38. D. V. Zhdanov and V. N. Zadkov, J. Chem. Phys. **127**, 244312 (2007).

39. D. V. Zhdanov and V. N. Zadkov, Phys. Rev. A **77**, R011401 (2008).

40. D. V. Zhdanov and V. N. Zadkov, Phys. Rev. A **78**, 033407 (2008).

41. P. A. L. Bachi-Tom, V. I. Tyulin, and V. K. Matveev, Rus. J. Phys. Chem. **73**, 1988 (1999).

42. J. Koput, S. Carter, and N. C. Handy, J. Chem. Phys. **115**, 8345 (2001).

43. B. A. Grishanin and V. N. Zadkov, JETPH **89**, 669 (1999).

44. S. S. Bychkov, B. A. Grishanin, V. N. Zadkov, and H. Takahashi, J. Raman Spectr. **33**, 962 (2002).

45. F. Hund, Z. Phys. **43**, 805 (1927).